J Nanostruct 9(2): 190-201, Spring 2019

RESEARCH PAPER

# Simultaneous Electrochemical Determination of Acetaminophen and Codeine Based on a MWCNT/MCM48 Nanocomposite Modified Glassy Carbon

*Ali Babaei* [1,2,*], *Sara Soleimani Babadi* [1] *and Masoud Sohrabi* [1]

[1] *Department of Chemistry, Faculty of Science, Arak University, Arak, Iran*

[2] *Institute of Nanosciences and Nanotechnology, Arak University, Arak, Iran*

**ARTICLE INFO**

***Article History:***
*Received 14 December 2018*
*Accepted 05 February 2019*
*Published 01 April 2019*

***Keywords:***
*Acetaminophen*
*Codeine*
*Multiwalled Carbon Nanotubes*
*MCM-48*

**ABSTRACT**

A novel chemically modified electrode was constructed based on multi-walled carbon nanotubes, MCM48 molecular sieve composite modified glassy carbon electrode .The modified electrode showed that it can be used for simultaneous determination of acetaminophen (ACT) and codeine (COD), simultaneously. The measurements were carried out by the application of differential pulse voltammetry (DPV), cyclic voltammetry (CV) and chronoamperometry (CA) methods. The fabricated sensor revealed some advantages such as excellent selectivity, good stability and high sensitivity toward ACT and COD determination. Application of DPV method under the optimum conditions showed the modified electrode provides linear responses versus ACT concentrations in the range of 0.2-40 μM and 80-350 μM. The results for COD showed the linear responses in the ranges of 4-70 μM and 150-400 μM respectively using DPV method. The modified electrode was used for determination of ACT and COD in real samples like human blood serum and plasma with satisfactory results.

**How to cite this article**
*Babaei A, Soleimani Babadi S, Sohrabi M. Simultaneous Electrochemical Determination of Acetaminophen and Codeine Based on a MWCNT/MCM48 Nanocomposite Modified Glassy Carbon. J Nanostruct, 2019; 9(2): 190-201.*
*DOI: 10.22052/JNS.2019.02.001*

## INTRODUCTION

Acetaminophen (N–acetyl–p–aminophenol, ACT) is among the most widely used medications as analgesic and antipyretic drugs [1]. It is remarkably safe in standard doses, however because of its wide availability, deliberate or accidental overdoses are not uncommon. Recent studies have shown that ACT is associated with hepatic toxicity and renal failure despite its apparent innocuous character [2].

Codeine (COD) is a natural opiates alkaloid from poppy or prepared from morphine by methylation [3]. Its phosphate form is usually used for the treatment of gently or moderate pain in clinic medication .It has similar applications to morphine, but with much less effect. COD is rapidly adsorbed from the gastrointestinal tract to be subsequently distributed through intravascular spaces to various body tissues, with preferential uptake by organs such as the liver, spleen and kidney [4].

The combination of ACT and COD is used to reduce fever and to relieve mild to moderate pain caused by a variety of conditions for example: headache, toothache, neuralgia, migraine and period pains. Also, the use of COD–containing products is strongly associated with endogenous depression, again a dual–diagnosis problem [5]. Since ACT and COD are commonly found in combination together in pharmaceutical formulations because the combination provides effective pain relief by

* *Corresponding Author Email: ali-babaei@araku.ac.ir*
*ali.babaei08@gmail.com*

about 40% higher than that offered by the same dose of ACT alone, so it is very important for the clinical laboratories and pharmaceutical industries to have a simple, fast and sensitive method [6]. Thus, numerous strategies have been reported for the determination ACT and COD, such as spectrophotometry [7], potentiometric titration [8], mass spectrometry [9] and high performance liquid chromatography [10]. These methods exhibit high sensitivity and selectivity, however, they are also time–consuming, high–cost, and require complicated sample pretreatments. In the past few decades, electrochemical methods have been received great attention because of their ease of monitoring, simplicity, high sensitivity and low cost [11-14].

Carbon nanotubes (CNTs), in forms of single–walled CNTs (SWCNTs) and multi–walled CNTs (MWCNTs), have specific properties such stability, and extreme mechanical strength [15-16]. Therefore, they have been used in various application fields including catalysis of redox reactions [17-18], nano-electronics [19] and electrochemical sensors [20-21]. Nowadays, carbon–based electrodes are widely used in electroanalytical chemistry, due to their broad potential window, rich surface chemistry and low background current and chemical inertness [22-23].

There are two well–defined porous adsorbents in the family of M41S materials. The first, MCM–41, has a hexagonal arrangement of unidirectional pores while the second, MCM–48, has a cubic structure indexed in the space group *Ia3d*, recently modelled as a gyroid minimal surface [24]. Interesting physical properties of MCM-48 are its high specific surface area up to 1600 $cm^2\ g^{-1}$, specific pore volume up to 1.2 $cm^3\ g^{-1}$ and high thermal stability [25]. MCM–48 seems to be a more interesting candidate as an adsorbent in separation techniques, for example, supercritical fluid chromatography, or as a catalyst support than MCM–41. This is because of its interwoven and branched pore structure, which provides more favorable mass transfer kinetics in catalytic and separation applications than MCM–41 with its unidirectional pore system. All published syntheses for MCM–48 proceed via the hydrothermal reaction [26]. In this work MCM-48 was used due to its high surface area and elevated porosity, so we expect its high ability to adsorb ACT and COD species on the modified electrode surface.

In the present study, a specific MWCNTs–MCM–48 nanocomposite modified glassy carbon electrode (MWCNTs–MCM–48/GCE) is developed and applied to achieve an extremely high active surface area for simultaneous electrochemical detection of ACT and COD.

According our knowledge there is no report on the application of MWCNTs– MCM–48/GCE for simultaneous electrochemical determination of ACT and COD. Therefore, the main target of this study is to develop a simple, sensitive and selective electrochemical sensor for the simultaneous determination of ACT and COD.

## EXPERIMENTAL

### *Materials and characterization*

All chemicals were analytical grade and were used without further purification. ACT and COD were obtained from Merck company. MWCNTs (>95 wt%, 5-20 nm) were purchased from Plasma Chem GmbH company. MWCNTs were used as they received. Stock standard solutions of 10 mM COD and 10 mM ACT was freshly prepared in 0.1 M phosphate buffers (PBS) of pH 7. ACT and COD solutions were prepared by diluting the stock standard solutions using 0.1 M phosphate buffer (pH=7). Buffer solutions in voltammetric studies were prepared as described elsewhere.

Fresh human blood serum and urine samples were obtained from Pars laboratory (Arak, Iran). The samples were filtered and diluted 50 times using a 0.1 M of PBS at pH 7, and used for the determinations of spiked ACT and COD.

### *Synthesis of MCM–48 nanoparticles*

MCM–48 was synthesized by the conventional hydrothermal pathway similar to the procedure that was described by Monnier et al.[27]. n–Hexadecyltrimethyl ammonium bromide ($C_{16}H_{33}(CH_3)_3$–NBr, template) was dissolved in deionized water, and sodium hydroxide and tetra ethoxysilane were added. The molar composition of the gel was 1 M of TEOS and 0.25M of $Na_2O$, 0.65 M of $C_{16}H_{33}(CH_3)_3$ NBr and 0.62M of $H_2O$. The solution was stirred for about 1 h, charged into a polypropylene bottle and then was heated at 110 $^0$C for 3 days. The product was filtered, washed with water and calcined at 550 $^0$C for 6 h to obtain MCM-48.

### *Instrumentation*

All the voltammetric measurements were carried out using MWCNTs–MCM–48/GCE as the working electrode, an Ag/ AgCl, KCl (3M) electrode

as the reference electrode and a platinum wire as an auxiliary electrode. Differential pulse voltammetry (DPV), cyclic voltammetry (CV) and chronoamperometry (CA) experiments were carried out using a Palm Sense instrument potentiostat (EcoChemie, The Netherlands). All potentials given are with respect to the potential of the reference electrode. The pH measurements were performed with a Metrohm 744 pH meter using a combination glass electrode. The morphological analyses were carried out using a Sigma VP Zeiss-scanning electron microscope (SEM).

*Preparation of MWCNTs–MCM–48/GC modified electrode*

Prior to use, GCE was first polished with alumina powder, rinsed thoroughly with doubly distilled water and dried at room temperature. A stock solution of MWCNTs– MCM–48 in DMF was prepared by dispersing appropriate weighed amounts of MWCNTs and MCM-48 (85:15 w/w) in 2 ml DMF using an ultrasonic bath until a homogeneous solution was resulted. Then 50 µL of prepared suspension was placed on the electrode with a microsyringe. This fabricated MWCNTs-MCM-48/GCE was placed in the electrochemical cell containing 0.1 M of PBS. Then 20 cycles in the potential window of 0.0 to 1.0 V were performed using the CV method to obtain stable responses.

*General procedure*

Each sample solution (10 mL) containing appropriate amounts of ACT and COD in 0.1 M PBS at pH 7, was transferred into the voltammetric cell. The voltammograms were recorded by applying a positive going potential from 0 to 1.1 V. The differential pulse voltammograms showed anodic peaks around 0.35 and 0.75 V corresponding to the ACT and COD compounds with current peaks being proportional to solution concentrations, respectively. Calibration curves were obtained by plotting the anodic peak currents of ACT and COD against the corresponding concentrations. All experiments were carried out under open circuit conditions. After each measurement, the MWCNTs–MCM–48/ GCE was regenerated by thoroughly washing the electrode with triply distilled water and then 2% sodium hydroxide solution. The electrode was finally rinsed carefully with distilled water to remove all adsorbates from the electrode surface and provide a fresh surface for the next experiment.

## RESULTS AND DISCUSSION

*Characterization of MWCNTs-MCM-48/GCE*

Fig. 1a and b. show typical SEM images of the MCM-48. The particles sizes of MCM-48 are between 20 to 40 nm lead to its high porosity and then large surface area. However, Fig. 1c, d, e, f, g and h show the SEM images of the MWCNTs-MCM-48 composite on the electrode. It can be seen MWCNT is well distributed on MCM-48. The fabricated composite could provide larger surface area with huge porosity characteristic which lead to therefore higher oxidation peak currents for ACT and COD could be obtained on the modified electrode with this composite. Energy dispersive X-ray (EDX) analysis of the MWCNTs-MCM-48 composite shows the presence of Si, O and C (Fig.1i). The presence of Si and O peaks beside of C peak confirms the successful modification of MWCNT with MCM-48.

*Cyclic voltammetry characterization of modified electrodes*

The electrochemical performance of MWCNTs and MWCNTs-MCM-48 modified GCE were investigated by using a solution of 5 mM $Fe[(CN)_6]^{3-}/^{4-}$ redox probe at scan rate of 0.08 V $s^{-1}$. As shown in Fig. 2 a pair of redox peaks with $\Delta E_p$ of0.153, 0.171and 0.35 were observed at MWCNTs-MCM-48 nanocomposite (solid line), MWCNTs (dashed line) modified GCE and bare GCE (dotted line), respectively. n order The higher peak currents and lower $\Delta E_p$, suggesting that MWCNTs-MCM-48/ GCE exhibits faster electron-transfer kinetics and larger electroactive surface area compared to bare glassy carbon electrode. In order to obtain those effects on the electrode quantitatively the ratio of the peak currents on the surface area of the MWCNTs and MWCNTs-MCM-48 nanocomposite modified electrodes were were compared with bare GCE, using 5mM $[Fe(CN)_6]^{3-}/^{4-}$ redox system and applying the Randles–Sevcik equation for a reversible process [28]:

$$I_P = (2.69 \times 10^5)\, A\, n^{3/2}\, D^{1/2}\, C_0\, v^{1/2} \qquad (1)$$

Where D and $C_0$ are the diffusion coefficient and bulk concentration of the redox system, respectively. The value n is the number of electron transferred (n = 1), $v$ is the scan rate and A is the

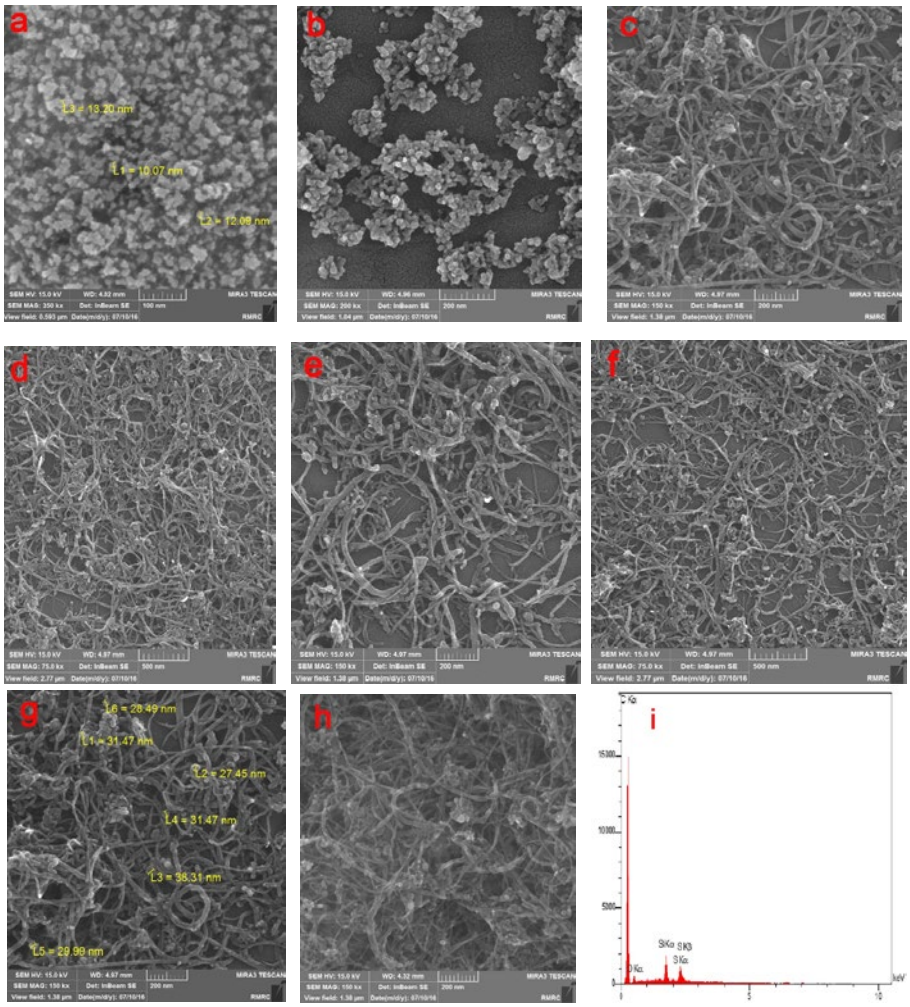


Fig1: a and b) SEM images of MCM-48, c,d,e,f,g and h) SEM images of the MWCNTs-MCM-48. i) EDX spectrum of MWCNTs-MCM-48.

effective surface area of the electrode. Cyclic voltammetry experiments at different scan rates were performed with the bare and modified glassy carbon electrodes immersed in the solution of $K_3[Fe(CN)_6]$. By plotting Ip respect to $v^{1/2}$ and comparing the slopes of the curves, the results showed the 20.5 and 14.5 times higher peak current for MWCNTs-MCM-48/GCE and MWCNTs/GCE respect to bare GCE, respectively.

*Effect of solution pH and supporting electrolyte*

Several buffers like PBS, ammonia, acetate and Britton Robinson (BR) were used as the supporting electrolyte in determinations of a 40 μM ACT and 100 μM COD solution using cyclic voltammetry(not shown). Well-defined peaks for ACT and COD were obtained in PBS with higher current responses compared to the others buffer. So PBS was chosen for further experiments.

The influence of the pH on the oxidation peak currents of ACT and COD were investigated in the pH range of 4-8 employing PBS, respectively (Fig. 3). According to Figs.3 (A) and (B), as the pH of the medium gradually increased, the oxidation potential of ACT and COD shifted toward less positive values, suggesting the involvement of protons in the reaction. In addition It was observed that the peak currents ($I_{pa}$) reached to their maximum values at pH 7 for ACT and COD oxidation. Thus, this pH was employed for further studies. Over the pH range of 4-8, the oxidation peak potentials ($E_{pa}$) were linear as a function of pH for ACT and COD, respectively. From the plot of $E_{pa}$ vs. pH, slopes of −0.062 V and −0.053 V were obtained for ACT and COD, corresponding to the following equations, respectively:

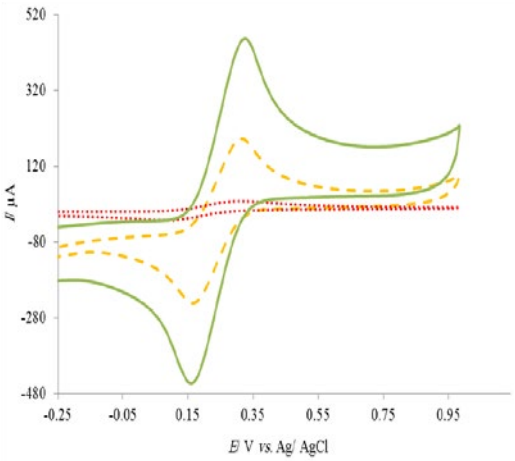


Fig. 2. Cyclic voltammograms of the GCE (dotted line), MWCNTs (dashed line) and MWCNTs-MCM-48 nanocomposite (solid line) glassy carbon electrodes in 5 mM $K_3[Fe(CN)_6]$, Scan rate: 0.08 V $s^{-1}$.

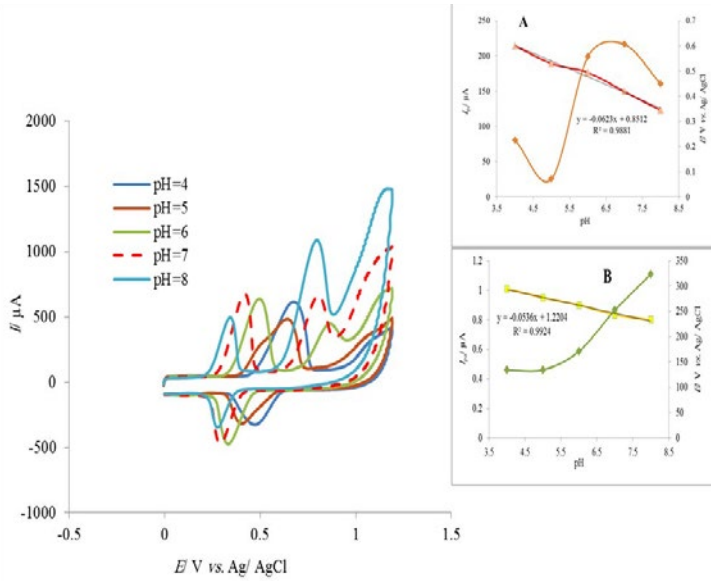


Fig.3. Cyclic voltammetry of MWCNTs-MCM48/GCE in 0.1 M PBS containing 40 µM of ACT and 100 µM of COD at different pH. Inset: dependence of peak potential and peak current (A: ACT, B: COD).

$E_{pa}$= −0.062pH + 0.8512; $R^2$=0.9881

$E_{pa}$= −0.053pH + 1.2204; $R^2$=0.9924

The slopes of the variations of $E_p$ as a function of solution pH are close to the Nernstian slope of 0.059, this result revealed that an equal number of protons and electrons were involved in the oxidation reactions of ACT and COD.

The possible reaction pathways for electro oxidation of ACT and COD on MWCNTs-MCM-48/GCE in 0.1 M phosphate buffered solution (pH 7) can be proposed as shown in Scheme 1.

*Effect of accumulation time*

The effect of accumulation time on the electrochemical response of the MWCNTs-MCM-48/GCE towards ACT and COD in the simultaneous determination of 40 µM ACT and 100 µM COD solution was investigated using the DPV method in PBS (pH=7) (not shown). The results show the corresponding oxidation peak currents of ACT and COD gradually increased by increasing accumulation time from 10 to 80s, and reached the maximum currents response at 40s. Further increasing the accumulation time, there is no significant increase in the current response. This phenomenon is probably

due to the saturated adsorption of ACT and COD on the MWCNTs-MCM-48/ GCE surface at such accumulation time. Therefore, an accumulation time of 40s was used for each voltammetric measurement of ACT and COD.

*DPV studies of Acetaminophen and Codeine on MWCNTs-MCM-48/GCE*

DPV response for the mixture of 100 µM ACT and COD(PBS, pH 7) at the GCE, MWCNT, and $MWCNT_S$-MCM-48 nanocomposite modified electrodes are shown in Fig.4. As can be seen, ACT and COD showed weak oxidation peaks at the bare glassy carbon electrode (dotted line) with oxidation potentials of 0.4 V and 0.8 V. In contrast, at MWCNTs modified electrode (dashed line), the peak currents increased and the anodic peak potential of ACT and COD were about 0.37 and 0.75, respectively. The slight shift and increase of the corresponding oxidation peaks of ACT and COD are due to electrocatalyttic effects and high surface area of MWCNTs. According to Fig. 4, the peak currents of ACT and COD at MWCNTs-MCM-48/GCE (solid line) showed higher oxidation peak currents for ACT and COD at the same potentials. These phenomena could be due high surface area and adsorption effect of MCM-48.. It is clear that the increase in oxidation current (compared with GCE), and well separation of the oxidation peak at proposed modified electrode can offer special approach for simultaneous and sensitive electrochemical determination of ACT and COD in the mixture solution at MWCNTs-MCM-48/GCE.

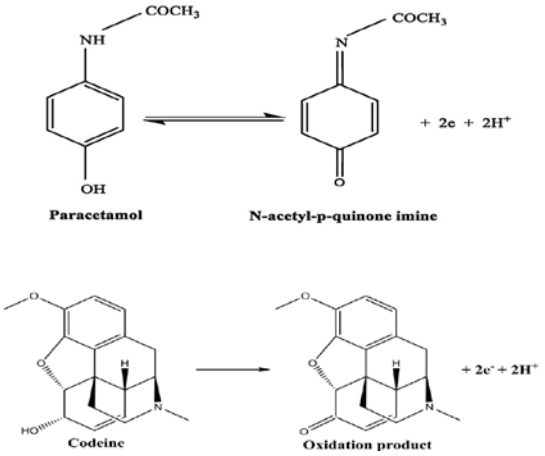


Scheme 1.The proposed oxidation reactions of ACT and COD.

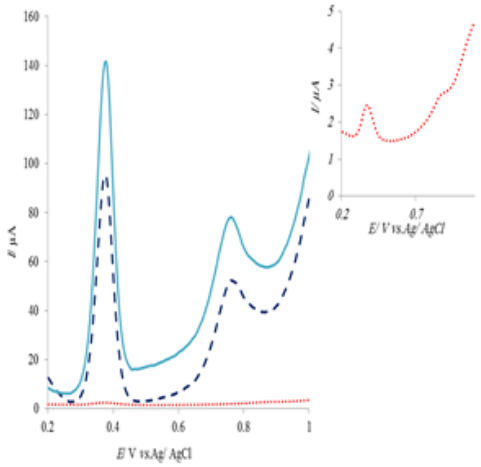


Fig. 4. DPV of MWCNTs-MCM48 nanocomposite (solid line), MWCNTs (dashed line) modified electrode and bare (dotted line) glassy carbon electrode in 0.1M PBS containing 20µM of ACT and 200µM COD.

*Effect of scanning rate*

The effect of scan rate on the electro-oxidations of ACT and COD at the MWCNTs-MCM-48/ GCE were investigated by CV to acquire information about electrochemical mechanism from the relationship between peak current and scan rate of potential.

The cyclic voltammograms of 100µM ACT and COD at MWCNTs-MCM-48/ GCE were recorded at different scan rates from 0.02 to 0.9 V $s^{-1}$ (not shown). The plot of peak height ($I_{pa}$) versus the square root of scan rate ($\upsilon^{1/2}$) in the range of 0.06–0.55 $Vs^{-1}$ was constructed for $1.0\times10^{-2}$M COD. The same diagram was obtained for $1.0\times10^{-2}$M ACT in the range of 0.02–0.6 V $s^{-1}$. The linear relationships were obtained for ACT and COD respectively, as follow:

$I_p(\mu A) = 1306.5\ \upsilon^{1/2}(V^{1/2}s^{-1/2}) - 155.58;\ R^2 = 0.9976$ (1)

$I_p(\mu A) = 499.24\upsilon^{1/2}\,(V^{1/2}\,s^{-1/2}) - 12.606;\ R^2 = 0.9949$ (2)

Suggesting that electrode process of ACT and COD were diffusion controlled. For diffusion controlled irreversible anodic reaction (e.g. COD), the peak potential, $E_p$, could be present by the following equation [29]:

$$E_p = E^0 - \left(\frac{RT}{\alpha_a nF}\right)\ln\left(\frac{RTk_s}{\alpha_a nF}\right) + \left(\frac{RT}{\alpha_a nF}\right)\ln\nu \qquad (3)$$

By drawing plots of Ep respect to logν as shown in Fig. 5 the values of α and $k_s$ can be calculated. The results of calculation for COD showed the values of $\alpha_a$ and $k_s$ equal to 0.52 and1.2 $s^{-1}$, respectively.

For a reversible system (e.g. ACT)based on Laviron theory the charge transfer coefficient (α) and electron transfer rate constant ($k_s$) can be determined by measuring the variation of $\Delta E_p$ *vs*. log scan rate. According to the slopes of $E_{pc}$ *vs*. log (ν) for ACT. and using the following equations the values of α could be obtained[31]:

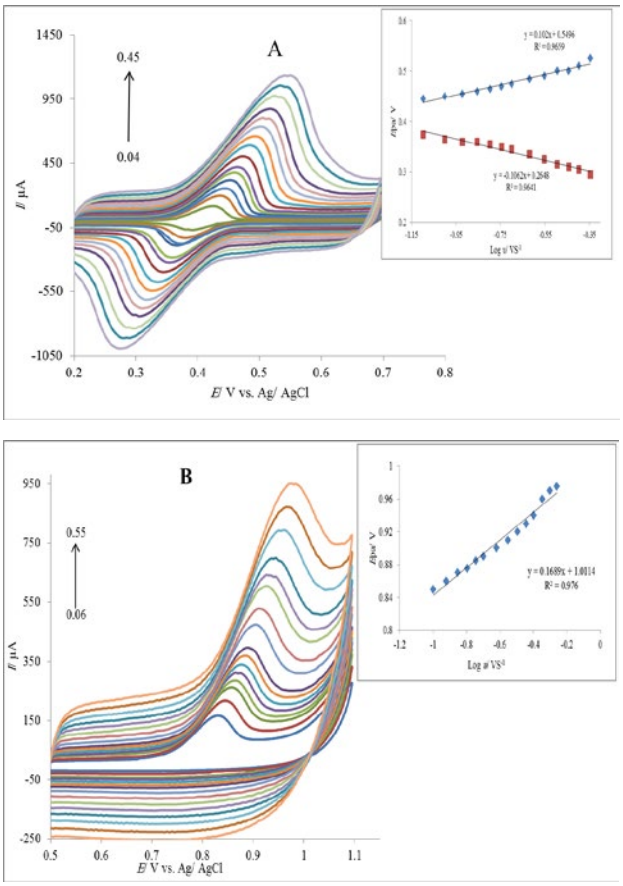


Fig. 5. Cyclic voltammograms of MWCNTs-MCM-48/ GCE in a 0.1 M PBS (pH 7) containing (A) ACT 100 µM, (B) COD 100 µM, (inset Dependence of peak potential, $E_{pa}$, on the logυ).

$$E_{pa} = E^{0'} + \frac{2.303RT}{(1-\alpha)nF}\log\upsilon + \frac{2.303RT}{(1-\alpha)nF}\log\frac{nF(1-\alpha)}{RTKs} \quad (4)$$

$$Epc = E^{0'} - \frac{2.303RT}{\alpha nF}\log\upsilon - \frac{2.303RT}{\alpha nF}\log\frac{\alpha nF}{RTKs} \quad (5)$$

$$log\ k_s = \alpha\ log(1-\alpha) + log\alpha - \log\frac{RT}{nF\upsilon} - \frac{\alpha(1-\alpha)nF}{2.3RT}\Delta Ep \quad (6)$$

By considering two electrons transferred for ACT, cathodic ($\alpha_c$) and anodic ($\alpha_a$) charge transfer coefficients of 0.4, 0.6 were obtained for ACT. By substituting these values in equation 6 the value of Ks was calculated to be 2.6. The large value of the electron transfer rate constant shows the high ability of the modified electrode for promoting electron transfer between the ACT and the electrode surface.

*Chronoamperometric study of Acetaminophen and Codeine*

Chronoamperometry study was utilized in the evaluation of the diffusion coefficient of ACT and COD. Fig.6. shows the chronoamperogram obtained using MWCNTs-MCM-48/ GCE in the presence of ACT and COD. The diffusion coefficient, *D*, for ACT and COD were determined using Cottrell equation:

$$I = n\ F\ D^{1/2}\ A\ C_0\ \pi^{-1/2}\ t^{-1/2} \quad (7)$$

Where *D* and $C_0$ are diffusion coefficient ($cm^2\ s^{-1}$) and the bulk concentration ($mol\ cm^{-3}$), respectively.

Under the diffusion control condition, a plot of *I vs.* $t^{-1/2}$ will be linear, and from the slope, the value

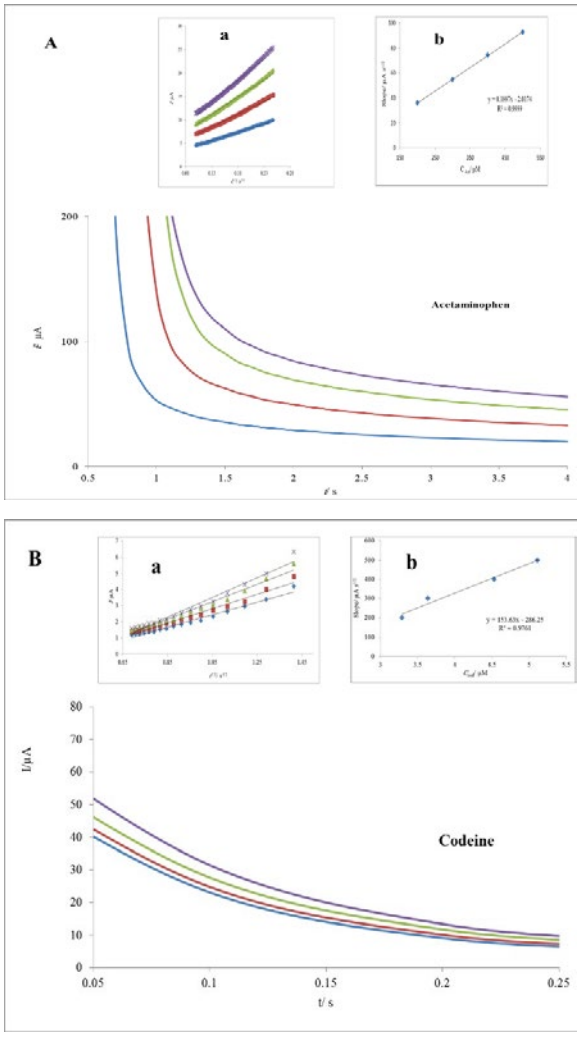


Fig. 6.chronoamperogram of MWCNTs-MCM-48/GCE at different concentrations; (A) ACT and (B) COD in a 0.1 M PBS (pH=7).Inset: (a) Cottrell plot and (b) linear dependence of Cottrell slopes versus concentration.

of *D* can be calculated. Fig. 6 (inset A) shows the experimental plots with the best fits for different concentrations of ACT, and COD employed. The slopes of the resulting straight lines were plotted *vs*. the analytes concentration (inset B of Fig. 6). The mean values of the *D* were estimated to be $7.58\times10^{-11}$ $cm^2$ $s^{-1}$ and $4.97\times10^{-5}$ $cm^2$ $s^{-1}$ for ACT and COD,respectively.

*Linear dynamic range and detection limit of the method*

The proposed method was employed for determination of ACT and COD in PBS at the optimum conditions. The experiments were carried out by variation of concentrations of analyte in the presence of the fixed concentration of the other. Fig. 7 shows DPV and the corresponding calibration curves obtained for various concentrations of ACT and COD at MWCNTs-MCM-48/ GCE. The anodic peak currents of ACT were proportional to the concentration in two concentration ranges of 0.2-40 µM with a calibration equation of:

$I_p$(µA) = 1.1882 C (µM) + 0.4203; $R^2$=0.9952,

and 80 - 350 µM with a calibration equation of:

$I_p$(µA) = 0.1555 C (µM) + 58.586; $R^2$=0.950.

In addition the obtained detection limit was 0.06 µM (S/N=3). For COD there were two linear dynamic ranges 4 to70 µM with a calibration equation of:

$I_p$(µA) = 0.5565C (µM)–0.2747; ($R^2$=0.981),

and 150- 400 µM with a calibration equation of:

$I_p$(µA) =0.0479 C (µM) + 48.729; ($R^2$=0.965). The detection limit of 0.9 µM (S/N = 3) was obtained.

Fig. 8. displays a chronoamperogram of the response of a rotated modified electrode (2500 rpm) following the successive injection of ACT and COD at the applied potential of 0.9 V in PBS (pH=7).

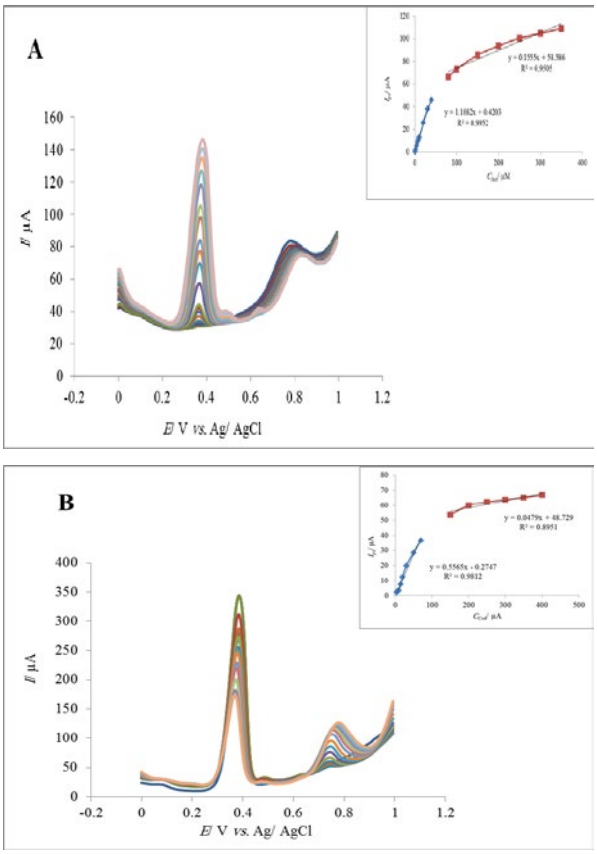


Fig. 7. DPV voltammograms obtained at the MWCNTs-MCM-48/GCE for (A) ACT at different concentrations in the presence of 400 µM COD .Inset: calibration curve of ACT and, (B) COD at different concentrations in the presence of 40µM ACT. Inset: calibration curve of COD.

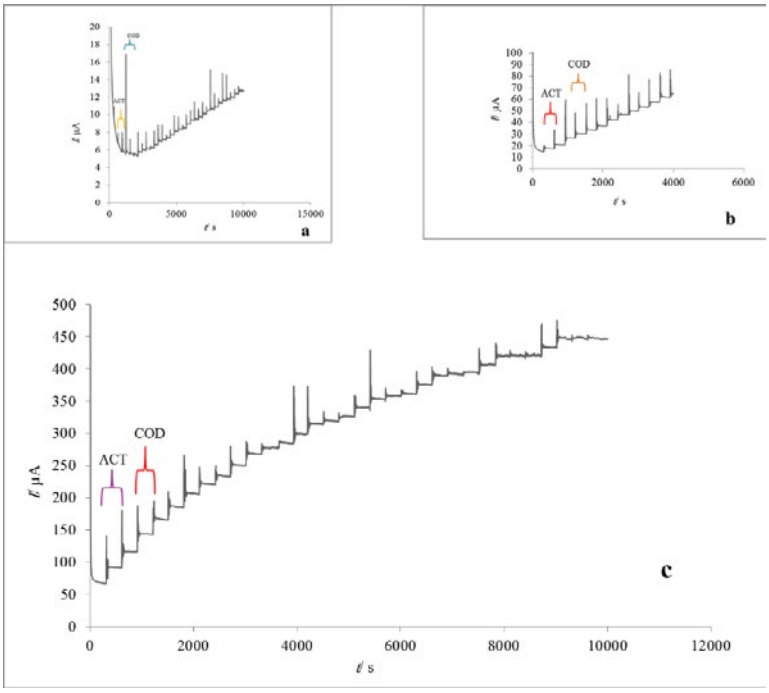


Fig. 8. Hydrodynamic Chronoamperometric response at rotating MWCNTs-MCM-48/GCE (rotating speed 2500 rpm) held at 0.90 V in PBS (pH 7) for simultaneous determination of ACT and COD by successive additions of: (a) 1 µM of ACT and COD ; (b) 12 µM of two analytes; (c) 96 µM of two analytes.

Table 1. Maximum tolerable concentration of interfering species.

| Interfering species | COD $C_{int}$ (µM)[a] | ACT $C_{int}$ (µM)[a] |
|---|---|---|
| Ascorbic acid | 1000 | 900 |
| L-Glutamic acid | 750 | 600 |
| L-Alanin | 450 | 500 |
| Aspartic acid | 550 | 450 |
| Tyrosine | 850 | 700 |

[a] Cint refers to interfering compound concentration.

ACT the linear dynamic range was from 1 - 472 µM, with a calibration equation of:

$I_p$ (µA) = 0.2776C (µM) +0.8855; $R^2$=0.9956 and a detection limit of 0.33 µM (S/N = 3). For COD the linear dynamic range was from 1–375 µM, with a calibration equation of:

$I_p$(µA) = 0.2931C (µM) + 0.6264 ($R^2$=0.9973) and a detection limit of 0.19 µM (S/N = 3).

*Repeatability and long-term stability of the electrode*

The repeatability of the method was studied by ten successive determinations of the 40 µM ACT and 100 µM COD solution using DPV method. The relative standard deviations (RSD) of 1.5% and 1.6% for ACT and COD were obtained, respectively. These small values indicate that the MWCNTs-MCM-48/ GCE is not subject to surface fouling by the oxidation products. The stability of MWCNTs-MCM-48-/ GCE was also explored. DPV experiments were carried out using the modified electrode that stored in solution or air for certain period of time. For example, in the determination of 40 µM ACT and 100µM COD in 0.1 M PBS (pH=7). When the modified electrode (after 10 h storage) was subjected to an experiment every 30 min, less than 8 and 10 % decrease in the oxidation peak currents of ACT and COD, respectively. When the electrode was stored in the atmosphere for 10 days, the oxidation peak currents of ACT and COD in the solution were reduced less than, 5.75 and 10.3 %, respectively. The results confirmed high stability of the proposed modified electrode.

Table 2. Determination of ACT and COD in human blood

| Sample | ACT added (μM) | COD added (μM) | ACT Found (μM) | ACT Recovery (%) | ACT RSD (%) | COD Found (μM) | COD Recovery (%) | COD RSD (%) |
|---|---|---|---|---|---|---|---|---|
| Blood Serum | – | – | <DL[a] | – | – | <DL | – | – |
| | 2.6 | 1.00 | 2.62±0.03 | 100.8 | 1.14 | 1.03±0.06 | 103 | 5.8 |
| | 25.0 | 3.00 | 25.2±0.26 | 100.8 | 1.03 | 2.88±0.16 | 96 | 5.5 |
| Blood Plasma | – | – | <DL | – | – | <DL | – | – |
| | 2.3 | 1.00 | 2.31±0.03 | 100.4 | 1.30 | 1.07±0.08 | 107 | 7.5 |
| | 25.0 | 3.00 | 24.97±0.42 | 99.9 | 1.68 | 3.13±0.15 | 104 | 4.7 |

[a] Average of five determinations at optimum conditions.

*Interference studies*

The effects of common interfering species in the presence of 20 μM ACT and 200μM COD by DPV under optimum conditions were investigated. Table 2 lists the tolerance limit for each potential interferent ,which is defined as the concentration of the interferent that gives an error of ≤10% in the determination of ACT or COD.

The results show that the proposed method is free from interferences of the most common interfering agents.

*Real sample analysis*

The human blood serum and plasma samples were diluted 100 times with PBS. Then various amounts of ACT and COD were spiked in the sample and then measured by DPV using MWCNTs-MCM-48/GCE at optimum conditions.

Concentrations were measured by applying the calibration plot using the standard addition method.

The results are summarized in Table 2. The good recovery values indicate good accuracy of the proposed method. The experimental results indicate that the proposed method has great potential for the determination of trace amounts of ACT and COD in biological systems or pharmaceutical preparations.

## CONCLUSION

In this work, a new application of a simple sensor based on multiwalled carbon nanotube and MCM-48 composite modified-glassy carbon electrode (MWCNTs-MCM-48/GCE) is introduced. The response of the MWCNTs–MCM-48/GCE for the simultaneous and single sensing of ACT and COD has been explored. The developed modified electrode exhibited remarkable increase in peak current and the electron transfer kinetics for electroactive compounds and decrease in the overpotential for the oxidation reaction of these compounds. The simple fabrication procedure, high speed, repeatability, high stability, wide linear dynamic range, high sensitivity, good selectivity and superior antifouling ability promote the proposed modified electrode is an attractive candidate for practical applications and to be an effective sensor for direct determination of ACT and COD in real sample.

## ACKNOWLEDGEMENT

The authors gratefully acknowledge the research council of Arak University for providing financial support (No. 95.2022) for this work.

## CONFLICT OF INTERESTS

The authors declare that there is no conflict of interests regarding the publication of this paper.

## REFERENCES

1. Williams LJ, Pasco JA, Henry MJ, Sanders KM, Nicholson GC, Kotowicz MA, et al. Paracetamol (acetaminophen) use, fracture and bone mineral density. Bone. 2011;48(6):1277-81.
2. Bosch ME, Sánchez AJR, Rojas FS, Ojeda CB. Determination of paracetamol: Historical evolution. Journal of Pharmaceutical and Biomedical Analysis. 2006;42(3):291-321.
3. Thorn CF, Klein TE, Altman RB. Codeine and morphine pathway. Pharmacogenetics and Genomics. 2009;19(7):556-8.
4. Caso JR, Lizasoain I, Lorenzo P, Moro MA, Leza JC. The role of tumor necrosis factor-alpha in stress-induced worsening of cerebral ischemia in rats. Neuroscience. 2006;142(1):59-69.
5. Garrido JMPJ, Delerue-Matos C, Borges F, Macedo TRA, Oliveira-Brett AM. Voltammetric Oxidation of Drugs of Abuse II. Codeine and Metabolites. Electroanalysis. 2004;16(17):1427-33.
6. Capella-Peiró M-E, Bose D, Rubert MF, Esteve-Romero J. Optimization of a capillary zone electrophoresis method by using a central composite factorial design for the determination of codeine and paracetamol in pharmaceuticals. Journal of Chromatography B. 2006;839(1-2):95-101.
7. Dogan HN, Duran A. Simultaneous spectrophotometric determination of aspirin, acetaminophen and ascorbic

acid in pharmaceutical preparations. Pharmazie. 1998;53(11):781-784.
8. Burgot G, Auffret F, Burgot JL. Determination of acetaminophen by thermometric titrimetry. Analytica Chimica Acta. 1997;343(1-2):125-8.
9. Nebot C, Gibb SW, Boyd KG. Quantification of human pharmaceuticals in water samples by high performance liquid chromatography–tandem mass spectrometry. Analytica Chimica Acta. 2007;598(1):87-94.
10. Talemi RP, Mashhadizadeh MH. A novel morphine electrochemical biosensor based on intercalative and electrostatic interaction of morphine with double strand DNA immobilized onto a modified Au electrode. Talanta. 2015;131:460-6.
11. Afsharmanesh E, Karimi-Maleh H, Pahlavan A, Vahedi J. Electrochemical behavior of morphine at ZnO/CNT nanocomposite room temperature ionic liquid modified carbon paste electrode and its determination in real samples. Journal of Molecular Liquids. 2013;181:8-13.
12. Ensafi AA, Ahmadi N, Rezaei B, Abarghoui MM. A new electrochemical sensor for the simultaneous determination of acetaminophen and codeine based on porous silicon/palladium nanostructure. Talanta. 2015;134:745-53.
13. Sanati AL, Karimi-Maleh H, Badiei A, Biparva P, Ensafi AA. A voltammetric sensor based on NiO/CNTs ionic liquid carbon paste electrode for determination of morphine in the presence of diclofenac. Materials Science and Engineering: C. 2014;35:379-85.
14. Wang S-C, Yang J, Zhou X-Y, Xie J, Ma L-L, Huang B. Electrochemical properties of carbon nanotube/graphene oxide hybrid electrodes fabricated via layer-by-layer self-assembly. Journal of Electroanalytical Chemistry. 2014;722-723:141-7.
15. Vukovi V, Vukovi B. AWGN Watermark in Images and E-Books - Optimal Embedding Strength. Watermarking - Volume 1: InTech; 2012.
16. Vairavapandian D, Vichchulada P, Lay MD. Preparation and modification of carbon nanotubes: Review of recent advances and applications in catalysis and sensing. Analytica Chimica Acta. 2008;626(2):119-29.
17. Gong K, Du F, Xia Z, Durstock M, Dai L. Nitrogen-Doped Carbon Nanotube Arrays with High Electrocatalytic Activity for Oxygen Reduction. Science. 2009;323(5915):760-4.
18. Wei B, Zhang ZJ, Ramanath G, Ajayan PM. Lift-up growth of aligned carbon nanotube patterns. Applied Physics Letters. 2000;77(19):2985-7.
19. Yang X, Feng B, He X, Li F, Ding Y, Fei J. Carbon nanomaterial based electrochemical sensors for biogenic amines. Microchimica Acta. 2013;180(11-12):935-56.
20. Rong L, Yang C, Qian Q, Xia X. Study of the nonenzymatic glucose sensor based on highly dispersed Pt nanoparticles supported on carbon nanotubes. Talanta. 2007;72(2):819-24.
21. Nemcova L, Barek J, Zima J. A voltammetric comparison of the properties of carbon paste electrodes containing glassy carbon microparticles of various sizes. Journal of Electroanalytical Chemistry. 2012;675:18-24.
22. McCreery RL. Advanced Carbon Electrode Materials for Molecular Electrochemistry. Chemical Reviews. 2008;108(7):2646-87.
23. Anderson MW. Simplified description of MCM-48. Zeolites. 1997;19(4):220-7.
24. Vartuli JC, Schmitt KD, Kresge CT, Roth WJ, Leonowicz ME, McCullen SB, et al. Development of a formation mechanism for M41S materials. Studies in Surface Science and Catalysis: Elsevier; 1994. p. 53-60.
25. Zhao D, Goldfarb D. Synthesis of mesoporous manganosilicates: Mn-MCM-41, Mn-MCM-48 and Mn-MCM-L. Journal of the Chemical Society, Chemical Communications. 1995(8):875.
26. Monnier A, Schuth F, Huo Q, Kumar D, Margolese D, Maxwell RS, et al. Cooperative Formation of Inorganic-Organic Interfaces in the Synthesis of Silicate Mesostructures. Science. 1993;261(5126):1299-303.
27. Goyal RN, Gupta VK, Chatterjee S. Voltammetric biosensors for the determination of paracetamol at carbon nanotube modified pyrolytic graphite electrode. Sensors and Actuators B: Chemical. 2010;149(1):252-8.
28. Zhao Y. Anodic oxidation of hydrazine at carbon nanotube powder microelectrode and its detection. Talanta. 2002;58(3):529-34.
29. Wu Y, Ji X, Hu S. Studies on electrochemical oxidation of azithromycin and its interaction with bovine serum albumin. Bioelectrochemistry. 2004;64(1):91-7.
30. Wang Z, Xia J, Zhu L, Chen X, Zhang F, Yao S, et al. A Selective Voltammetric Method for Detecting Dopamine at Quercetin Modified Electrode Incorporating Graphene. Electroanalysis. 2011;23(10):2463-71.